

# A first look at open charm production in Indium-Indium collisions at SPS energies

The NA60 Collaboration

R. Shahoyan<sup>2,5,a</sup>, R. Arnaldi<sup>9</sup>, R. Averbeck<sup>11</sup>, K. Banicz<sup>2,4</sup>, J. Castor<sup>3</sup>, B. Chaurand<sup>7</sup>, C. Cicalo<sup>1</sup>, A. Colla<sup>9</sup>, P. Cortese<sup>9</sup>, S. Damjanovic<sup>4</sup>, A. David<sup>2,5</sup>, A. de Falco<sup>1</sup>, A. Devaux<sup>3</sup>, A. Drees<sup>11</sup>, L. Ducroux<sup>6</sup>, H. En'yo<sup>8</sup>, A. Ferretti<sup>9</sup>, M. Floris<sup>1</sup>, P. Force<sup>3</sup>, N. Guettet<sup>2,3</sup>, A. Guichard<sup>6</sup>, H. Gulkanian<sup>10</sup>, J. Heuser<sup>8</sup>, M. Keil<sup>2,4</sup>, L. Kluberg<sup>2,7</sup>, J. Lozano<sup>5</sup>, C. Lourenço<sup>2</sup>, F. Manso<sup>3</sup>, A. Masoni<sup>1</sup>, P. Martins<sup>2,5</sup>, A. Neves<sup>5</sup>, H. Ohnishi<sup>8</sup>, C. Oppedisano<sup>9</sup>, P. Parracho<sup>2</sup>, P. Pillot<sup>6</sup>, G. Puddu<sup>1</sup>, E. Radermacher<sup>2</sup>, P. Ramalhete<sup>2,5</sup>, P. Rosinsky<sup>2</sup>, E. Scomparin<sup>9</sup>, J. Seixas<sup>2,5</sup>, S. Serci<sup>1</sup>, P. Sonderegger<sup>5</sup>, H.J. Specht<sup>4</sup>, R. Tieulent<sup>6</sup>, G. Usai<sup>1</sup>, R. Veenhof<sup>2,5</sup>, H.K. Wöhri<sup>2,5</sup>

<sup>1</sup> Università di Cagliari and INFN, Cagliari, Italy

<sup>2</sup> CERN, Geneva, Switzerland

<sup>3</sup> LPC, Université Blaise Pascal and CNRS-IN2P3, Clermont-Ferrand, France

<sup>4</sup> Universität Heidelberg, Heidelberg, Germany

<sup>5</sup> IST-CFTP, Lisbon, Portugal

<sup>6</sup> IPN-Lyon, Université Claude Bernard Lyon-I and CNRS-IN2P3, Lyon, France

<sup>7</sup> LLR, Ecole Polytechnique and CNRS-IN2P3, Palaiseau, France

<sup>8</sup> RIKEN, Wako, Saitama, Japan

<sup>9</sup> Università di Torino and INFN, Italy

<sup>10</sup> YerPhI, Yerevan, Armenia

<sup>11</sup> SUNY Stony Brook, New York, USA

Received: 16 February 2005 / Revised version: 28 February 2005 /

Published online: 2 August 2005 – © Springer-Verlag / Società Italiana di Fisica 2005

**Abstract.** NA60 is an experiment at the CERN-SPS devoted to the study of dimuon production in heavy-ion and proton-nucleus collisions. The main topics under study are low mass vector meson production,  $J/\psi$  production and suppression, and the sources of the dimuon continuum in the mass range  $1.2\text{--}2.7\text{ GeV}/c^2$ . In 2003, NA60 collected  $\sim 230$  million dimuon events from Indium-Indium collisions. We present preliminary results of the analysis of this data sample in view of measuring the open charm contribution to the dimuon spectrum. Although we are still working on the final background subtraction procedure, we can already demonstrate that the detector performance is good enough to allow the separation of prompt dimuons from muon pairs originating in distant  $D\bar{D}$  decays.

**PACS.** 25.75.Dw, 25.75.Nq

## 1 Introduction

The study of dimuon production in heavy-ion collisions is generally considered to be one of the most powerful tools in the search for the phase transition between the normal nuclear matter and the Quark-Gluon Plasma phase, where the quarks and gluons are no longer confined into hadrons. The most intriguing findings of dilepton experiments working in this field have been: the excess in the production of dielectron pairs in the mass window  $200\text{--}700\text{ MeV}$ , together with the flattening of the  $\rho$  and  $\omega$  peaks, observed by the NA45/CERES experiment in S-Au and Pb-Au collisions [1]; the anomalous  $J/\psi$  suppression found by NA50 in central Pb-Pb collisions [2]; and the

excess in the production of dimuons in the “intermediate mass region”,  $1.2\text{--}2.7\text{ GeV}/c^2$ , seen by NA38 and NA50 in S-U and Pb-Pb collisions [3], and by HELIOS-3 in S-W [4].

This paper addresses the last point. The continuum between the  $\phi$  and  $J/\psi$  peaks is well described in p-A collisions by the superposition of Drell-Yan dimuons and muon pairs from simultaneous semi-muonic decays of D and  $\bar{D}$  mesons [3]. Since the Drell-Yan contribution can be normalized from the high mass region, an excess in heavy-ion collisions is more likely to be due to the increase of *open charm* production (which is non-trivial to explain in the framework of perturbative QCD) or to the appearance of the long-sought *thermal dimuons*, considered to be one of the most direct signatures of QGP formation [5].

In order to measure the open charm contribution to the dimuon spectrum, NA60 exploits the long lifetime of

<sup>a</sup> e-mail: ruben.shahoyan@cern.ch

D mesons:  $c\tau = 312\mu\text{m}$  for  $D^+$  and  $123\mu\text{m}$  for  $D^0$  [6]. By selecting those muon pairs in which both muons are offset from the interaction vertex by more than a certain value, we can strongly suppress the prompt contribution, thus enriching the open charm fraction. Conversely, by selecting only muons with small offsets, we can obtain a sample dominated by prompt dimuons. Since the typical offset of the muon is equal to  $c\tau$ , such a selection requires the knowledge of both the interaction vertex position and of the muons' offsets with a precision of  $\sim 50\mu\text{m}$ , or better.

## 2 Experimental setup

The NA60 setup consists of a Muon Spectrometer and a Zero Degree Calorimeter, both inherited from NA50, a Vertex Telescope made from Silicon pixel planes, and a Beam Tracker (BT) measuring the transverse position of the incoming ion before its interaction in the target. A global description of the experimental apparatus is given in [7]; the Vertex Telescope is described in [8].

The essential feature of NA60 is the matching between the muons reconstructed in the Muon Spectrometer and the tracks measured in the Vertex Telescope before they scatter in the hadron absorber. This is done by computing the weighted distance squared ( $\chi^2$ ) between these two tracks in the space of angles and inverse momenta, taking into account the error matrix of the kinematics fits. In spite of the high occupancy in the vertex region, the excellent angular resolution of the Vertex Telescope (better than 1 mrad) results in a good enough separation between correct and fake matches, i.e. associations of the muons to wrong tracks in the Vertex Telescope. Figure 1 shows the shapes of the matching  $\chi^2/\text{NDF}$  distributions for correct and fake associations.

The matching procedure greatly improves the mass resolution: at the  $\omega$  mass it changes from 70–80  $\text{MeV}/c^2$  in NA50 to 20–25  $\text{MeV}/c^2$  in NA60. Furthermore, it allows us to relate the muon to the interaction vertex, something impossible in NA50. This improves the kinematics of the measured muons and strongly reduces the level of back-

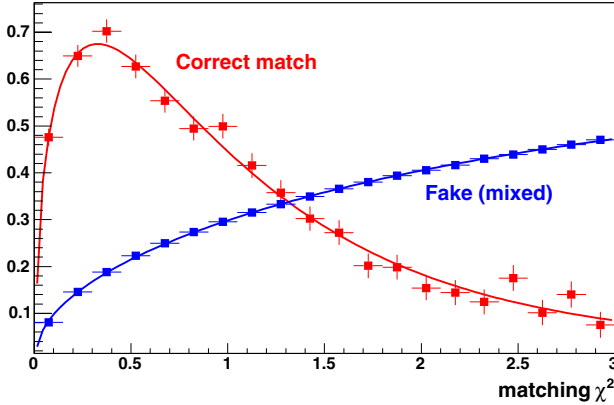


**Fig. 1.** Distribution of the matching  $\chi^2/\text{NDF}$  for correct and accidental associations between the muon and the track in the vertex region (normalized to unit areas)

ground muons originating from  $\pi$  and  $K$  decays. The following sections describe the background subtraction procedure and discuss the performance of the detector.

## 3 Background subtraction

There are two kinds of background in the data of NA60. The first one, the *combinatorial background*, is due to muons from uncorrelated decays of pions and kaons. In order to estimate this contribution, NA60 collected like-sign dimuon data in addition to the  $\mu^+\mu^-$  events. The subtraction of the combinatorial background is done using a *mixed-event technique*, combining into muon pairs two single muons from different like-sign dimuon triggers, in such a way that the obtained dimuons take into account the acceptance and trigger conditions of NA60. Figure 2 shows the measured opposite-sign and the generated background dimuon spectra, together with the “signal” obtained after background subtraction.

In order to control the quality of the *mixed* combinatorial background, we also generate like-sign pairs together with the opposite-sign dimuons. The comparison of the

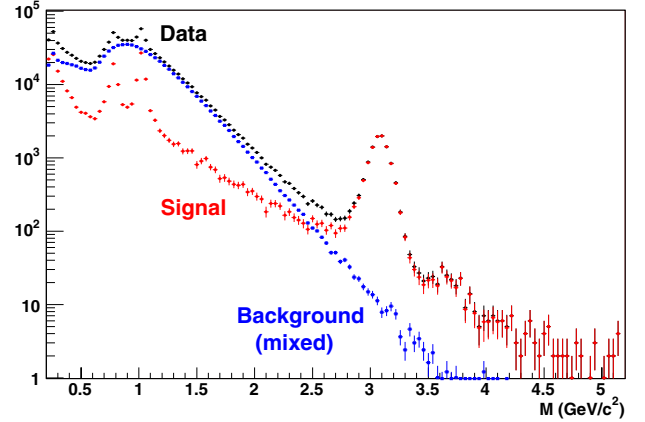


**Fig. 2.** Dimuon mass distributions of the measured  $\mu^+\mu^-$  pairs, of the generated *mixed* dimuons, and of the “signal”, obtained after combinatorial background subtraction

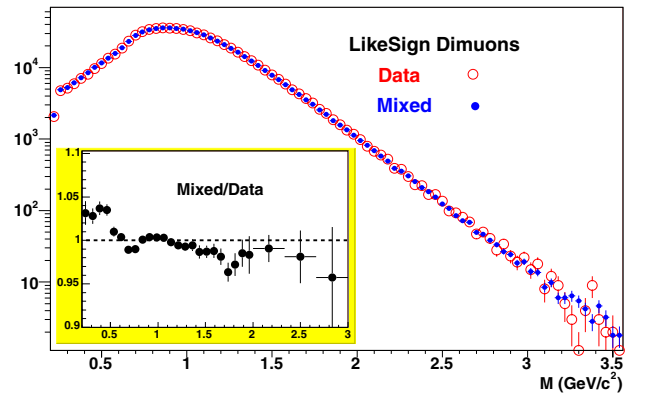


**Fig. 3.** Measured and generated like-sign combinatorial background spectra. The insert shows the ratio between mixed and measured distributions

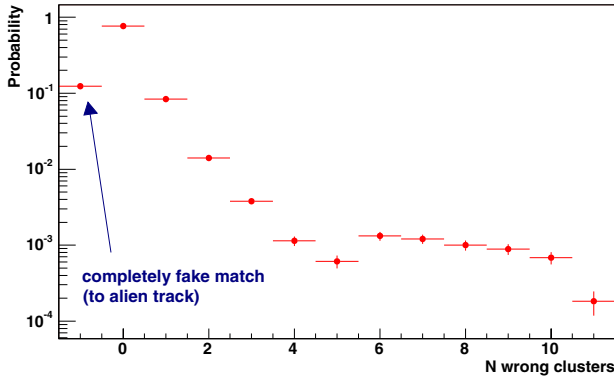


**Fig. 4.** Probability of matching a muon from the Muon Spectrometer to the right track in the Vertex Telescope versus the number of non-muon hits in this track. The first point corresponds to tracks with no hit in common with the muon

generated and measured like-sign spectra, shown in Fig. 3, demonstrates that this technique provides  $\sim 1\%$  precision over four orders of magnitude.

The second type of background is due to *fake matches* between the muons from the spectrometer and tracks in the vertex telescope. Occasionally, instead of the correct muon track in the vertex telescope, an accidental hadronic track is picked because it happens to be closer to the extrapolated Muon Spectrometer track. Apart from purely fake matches (i.e. when the selected track has nothing to do with the muon), we can also select a track made of some hits from the muon and some hits from other particles. Figure 4 shows the probability of such a match as a function of the number of non-muon hits in the matched track. The leftmost point corresponds to the case when the muon is matched to a purely hadronic track. At the dimuon level, and integrating over all collision centralities, the contribution of fake matches is  $\sim 20\%$  under the  $\phi$  peak, and drops to negligible values under the  $J/\psi$ .

The subtraction of this kind of background, using the mixed-event technique, is currently under study. Therefore, the qualitative results presented here were obtained without subtracting the fake match contribution.

## 4 Vertex resolution

The vertex reconstruction is done using a robust algorithm similar to the one presented in [9], modified to take into account the presence of our magnetic field. It can resolve multiple vertices, provided they are in different targets, and provides good target identification even for very peripheral collisions, down to  $N_{\text{tracks}} \geq 4$ . Figure 5 shows the  $Z$  coordinate (beam direction) of the reconstructed vertices passing the selection cuts used in this analysis. Apart from the seven Indium targets, we clearly see the peaks corresponding to the vacuum windows and to the downstream station of the Beam Tracker, with vertices reconstructed in its two microstrip sensors.

In order to control the resolution of the fitted vertices, we can extrapolate the beam track from the Beam Tracker,

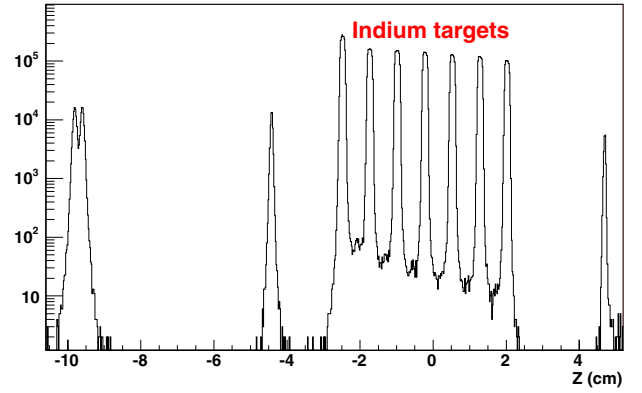


**Fig. 5.** Distribution of the  $Z$  coordinate (beam direction) of the reconstructed vertices. The first peak corresponds to the downstream tracking station of the Beam Tracker

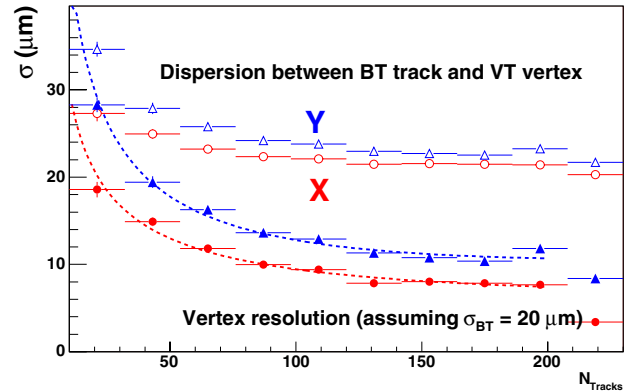


**Fig. 6.** Dispersion between the fitted vertex and the Beam Tracker prediction (open symbols) and extracted vertex resolution (closed symbols), assuming a BT precision of  $20\ \mu\text{m}$

with a precision of  $\sim 20\ \mu\text{m}$  at the targets, independently of collision multiplicity. Figure 6 shows the dispersion between the transverse position of the fitted vertex and of the Beam Tracker prediction, as a function of the number of tracks associated with the vertex. For most of our data, the extracted vertex resolution is better than  $10\ \mu\text{m}$  in  $X$  (bending plane) and better than  $15\ \mu\text{m}$  in  $Y$ .

## 5 Offset resolution

We define *offset* as the difference between the transverse coordinates of the vertex and of the muon track, evaluated to the  $Z$  coordinate of the vertex. Both vertexing and track fit errors contribute to the offset resolution. Due to the considerable amount of multiple scattering ( $\sim 2\% X_0$  per pixel plane), the error of the muon track extrapolation strongly depends on its momentum. In order to estimate the offset resolution we use the  $J/\psi$  muons, which are supposed to come exactly from the interaction point.

Figure 7 shows the offset resolution measured for  $J/\psi$  muons as a function of their inverse momentum. Expected values from Monte Carlo simulations are also shown. With the detection efficiencies of the pixel detectors still under

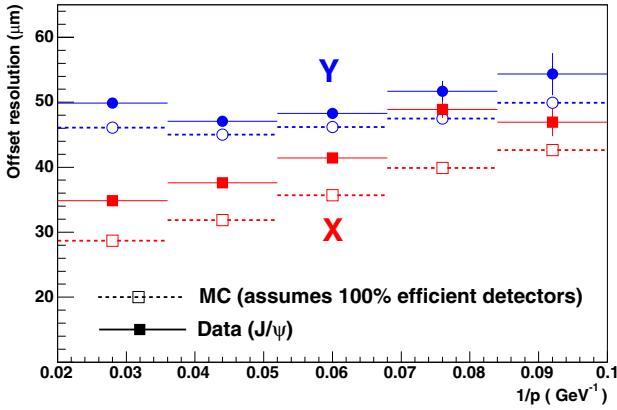


**Fig. 7.** The measured offset resolution for  $J/\psi$  muons (solid symbols) compared to the values expected from a Monte Carlo simulation, assuming fully efficient pixels (open symbols)

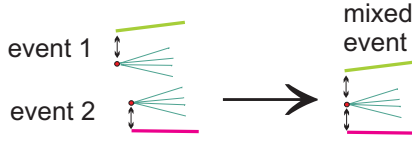


**Fig. 8.** Muons picked from different events keep the offsets with respect to their original vertices

evaluation, 100% efficiency was assumed in the simulation. More realistic efficiencies should remove the small discrepancy between measured and expected values.

In order to take into account the dependence of the muon offset resolution on its momentum, the measured offsets are weighted by the inverse of their covariant error matrices,  $V^{-1}$ , which incorporate the uncertainties from the vertex fit and from the muon extrapolation,

$$\Delta = \sqrt{\Delta x^2 V_{xx}^{-1} + \Delta y^2 V_{yy}^{-1} + 2\Delta x \Delta y V_{xy}^{-1}}$$

Since the combinatorial background muons originate from decays far from the interaction point, they strongly contribute to the offset range of a few hundred microns, where we expect the open charm signal. Thus, special care must be taken when building the mixed pairs for the background subtraction. In particular, we have to ensure that the muons of the final *mixed* event will have the same offsets, with respect to a randomly selected “interaction vertex”, as they have in the events where they were picked from for mixing. This procedure is illustrated in Fig. 8.

Figure 9 shows that the measured and mixed like-sign offset distributions agree with each other within a few percent. One should note that the fake muon matches have a considerably worse offset resolution. Figure 10 shows the weighted offset distribution from a Monte Carlo simulation of  $D\bar{D}$  and Drell-Yan muons (normalized to unit area). The fake match contribution to each spectrum is shown separately in open symbols. The insert shows the relative fraction of fake matches, for each process, confirming that the fake matches contribute mostly to the events with relatively high offsets. The resolving power of the offset cuts will significantly improve once the fake match subtraction is implemented.

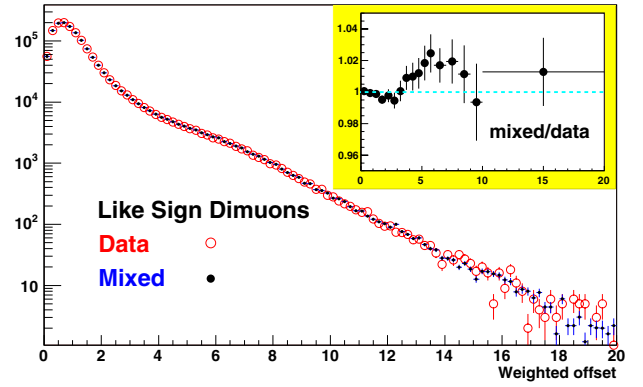


**Fig. 9.** Weighted offset distributions for muons from like-sign *mixed* (closed circles) and measured (open circles) event samples. The insert shows their ratio

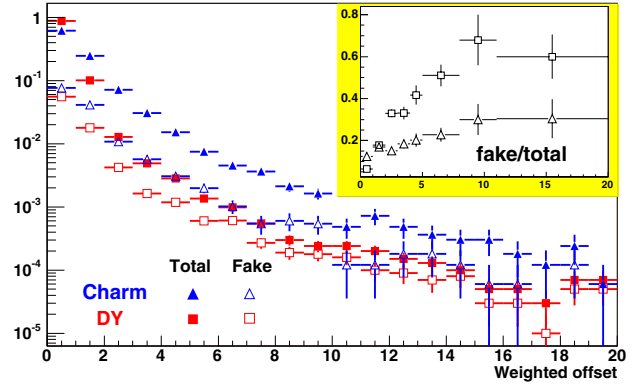
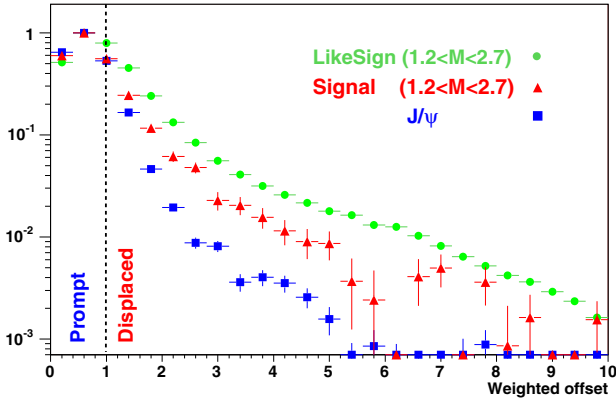


**Fig. 10.** Expected weighted offset distribution for open charm (closed triangles) and Drell-Yan (closed squares) muons, normalized to unit area. The fake match contribution is shown in open symbols. The fraction of fake match contribution, for each signal, is shown in the insert

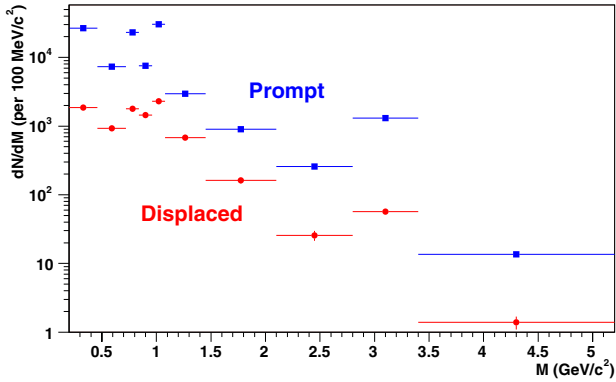
## 6 Results

Figure 11 shows the weighted offset distributions for three event samples:  $J/\psi$  dimuons, signal dimuons in the mass range  $1.2\text{--}2.7\text{ GeV}/c^2$ , and like-sign muon pairs in the same mass window.

In order to separate the open charm contribution from the prompt dimuons, we adopted the following procedure. First, dimuons with both muons having weighted offsets above 1 (corresponding to a distance of  $\sim 90\ \mu\text{m}$  for muons with momenta around  $15\text{ GeV}/c$ ) are attributed to the “displaced sample”, otherwise they are labeled as “prompt”. The dashed line in Fig. 11 shows the position of this selection cut. This selection, on its own, is affected by events where the vertex is poorly reconstructed, or the offsets were computed with respect to a wrong vertex. This problem is minimized by introducing a second selection cut, based on the weighted transverse distance,  $\Delta_{\mu\mu}$ , between the two muons extrapolated to the  $Z$  position of the vertex: the “displaced” events are only kept if  $\Delta_{\mu\mu} > 0.7$ , while the “prompt” dimuons must have  $\Delta_{\mu\mu} < 2$ , to be validated. The resulting mass spectra for the “displaced” and “prompt” selections are shown in Fig. 12.



**Fig. 11.** Distributions of the weighted offsets for three event classes:  $J/\psi$  dimuons, signal and like-sign dimuons in the 1.2–2.7  $\text{GeV}/c^2$  mass range. The dashed line signals the value of the selection cut



**Fig. 12.** Mass spectra corresponding to “prompt” (top) and “displaced” (bottom) selections

Notice that the regions dominated by the  $\omega$ ,  $\phi$  and  $J/\psi$  peaks are strongly suppressed in the “displaced” sample. This is better seen in Fig. 13, which shows the ratio between displaced and prompt spectra: clear minima are seen in the mass ranges dominated by the resonances.

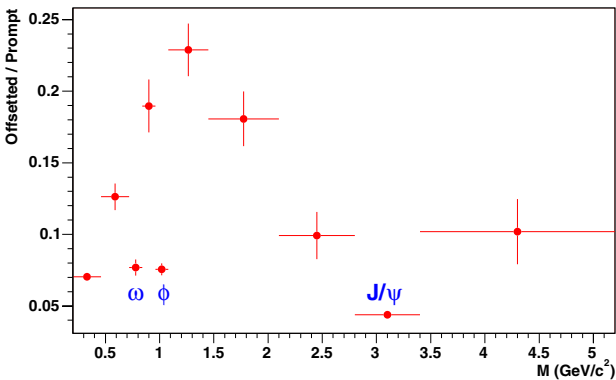


**Fig. 13.** Ratio between the “displaced” and “prompt” dimuon mass spectra

## 7 Conclusions

The preliminary results presented in this paper correspond to  $\sim 20\%$  of the In-In data collected in 2003. Although the fake match background subtraction is still under study, and has not been used in the analysis presented here, we have demonstrated that the detector performance meets the expectations. Even without the full background subtraction, the application of the offset cut allows us to separate the contributions of prompt and displaced events in the measured dimuon spectrum. The study of In-In data should be complemented by a similar analysis of the reference proton-nucleus collision data. In 2004, NA60 collected proton-nucleus data at 400 GeV (with a short period at 158 GeV), using Be, Al, Cu, In, Pb, W and U targets. According to preliminary estimates, around 300 000  $J/\psi$  dimuons were collected (before matching to the Vertex Telescope), and a similar amount of open charm muon pairs are expected in the mass range 1.2–2.7  $\text{GeV}/c^2$ .

*Acknowledgements.* Zheng Li developed and produced the silicon sensors of the Beam Tracker at BNL and Kurt Borer built the corresponding read-out electronics chain at LHEP, Bern. The ALICE pixel team helped in the development of our silicon pixel telescope. Many other people contributed to the feasibility of our experiment, including L. Casagrande, B. Cheynis, E. David, J. Fargeix, W. Flegel, L. Gatignon, V. Granata, J.Y. Grossiord, F. Hahn, S. Haider, L. Kottelat, D. Marras, I. McGill, T. Niinikoski, R. Oliveira, A. Onnela, V. Palmieri, J.M. Rieubland, J. Rochez, M. Sanchez, and H. Vardanyan. This work was partially supported by the Fundação para a Ciência e Tecnologia, Portugal.

## References

1. G. Agakichiev et al. (CERES Coll.), Phys. Rev. Lett. **75**, 1272 (1995); Phys. Lett. B **422**, 405 (1998); B. Lenkeit et al. (CERES Coll.), Nucl. Phys. A **661**, 23c (1999)
2. B. Alessandro et al. (NA50 Coll.), Eur. Phys. J. C **39**, 335 (2005); M. Balit et al. (NA50 Coll.), Phys. Lett. B **140**, 337 (1997)
3. M.C. Abreu et al. (NA50 Coll.), Eur. Phys. J. C **14**, 443 (2000)
4. A.L.S. Angelis et al. (HELIOS-3 Coll.), Eur. Phys. J. C **13**, 433 (2000)
5. R. Rapp, E. Shuryak, Phys. Lett. B **473**, 13 (2000)
6. S. Eidelman et al. (PDG), Phys. Lett. B **592**, 1 (2004)
7. R. Arnaldi et al. (NA60 Coll.), EPJ C **43** (2005)
8. K. Banicz et al., Nucl. Instrum. Meth. A **539**, 137 (2005)
9. G. Agakichiev et al., Nucl. Instrum. Meth. A **394**, 225 (1997)